Astrophys Space Sci (2006) 302:243–251
DOI 10.1007/s10509-006-9049-4

ORIGINAL ARTICLE

Formation of Small-Scale Condensations in the Molecular Clouds via Thermal Instability

Mohsen Nejad-Asghar · Jamshid Ghanbari

Received: 29 May 2004 / Accepted: 7 March 2006

Abstract A systematic study of the linear thermal instability of a self-gravitating magnetic molecular cloud is carried out for the case when the unperturbed background is subject to local expansion or contraction. We consider the ambipolar diffusion, or ion-neutral friction on the perturbed states. In this way, we obtain a non-dimensional characteristic equation that reduces to the prior characteristic equation in the non-gravitating stationary background. By parametric manipulation of this characteristic equation, we conclude that there are, not only oblate condensation forming solutions, but also prolate solutions according to local expansion or contraction of the background. We obtain the conditions for existence of the Field lengths that thermal instability in the molecular clouds can occur. If these conditions establish, small-scale condensations in the form of spherical, oblate, or prolate shape may be produced via thermal instability.

Keywords ISM: clouds · ISM: molecules · ISM: structure · Instabilities · Star: formation

1. Introduction

With the increase in the observational resolution, smaller sizes of density fluctuations have been detected. Direct imaging of ^{12}CO in nearby clouds revealed substructures with scales of $\sim 0.01 pc$ ($\sim 0.01 M_{\odot}$) (Peng et al., 1998; Sakamoto and Sunada, 2003). Studies of the time variability of absorption lines indicates the presence of small-scale clumps in the dense gas on scales so small as $\sim 5 \times 10^{-5} pc$ ($\sim$10AU), with masses of $\sim 5 \times 10^{-9} M_{\odot}$ (Moore and Marscher, 1995; Rollinde et al., 2003).

As a general rule, neither subparsec nor AU-scale condensations in molecular clouds are spherical (Ryden, 1996). Jones and Basu (2002) have recently decipher intrinsic three-dimensional shape distributions of molecular clouds, cloud cores, Bok globules, and condensations. They find out that molecular clouds mapped in ^{12}CO are intrinsically triaxial but more nearly prolate than oblate, while the smaller cloud cores, Bok globules, and small-scale condensations are also intrinsically triaxial but more nearly oblate than prolate.

Small-scale condensations appear to be immediate precursor of large-scale clumps (dense cores with significant Jeans mass) via merging and collisions; they constitute the initial conditions for star formation. Therefore, the understanding of the origin and merging of these small-scale condensations is of fundamental importance for a consistent theory of star formation and galactic evolution.

The origin and shape of these small-scale condensations is a disputable issue. Anisotropic heating and fragmentation via gravitational collapse is an important reason for oblate/prolate large-scale clumps with significant Jeans mass (e.g. Nelson and Langer, 1997; Indebetouw and Zweibel, 2000; Hartmann, 2002). The above scenario is not correct for small-scale condensations, because they have low gas density and small sizes, thus, their masses are significantly smaller than their corresponding Jeans mass. According to this feature, the only remaining responsible parameters may be *turbulence* and/or *thermal instability*.

Gammie et al. (2003) have recently studied the effect of turbulence in three dimensional analogs of clumps using a set of self consistent, time-dependent, numerical models of molecular clouds. The models follow the decay of initially supersonic turbulence in an isothermal, self-gravitating,

M. Nejad-Asghar (✉)
School of Physics, Damghan University of Basic Sciences, Iran
e-mail: nasghar@dubs.ac.ir

J. Ghanbari
Department of Physics, Ferdowsi University, Mashhad, Iran

magnetized fluid. They have concluded that nearly 90% of the clumps are formed in prolate and 10% of them are oblate.

In molecular clouds, the dispersion velocity inferred from molecular line width is often larger than the gas sound speed inferred from transition temperatures (Solomon et al., 1987). Magnetohydrodynamic turbulence may be responsible for the stirring of these clouds (Arons and Max, 1975). Because of these turbulent motions, molecular clouds must be transient structures, and are probably dispersed after not much more than $\sim 10^7 yr$ (Larson, 1981). Since cooling time-scale of molecular clouds is approximately $\sim 10^3 - 10^4 yr$ (Gilden, 1984), thermal instability may be a coordinated trigger mechanism to form condensations. Turbulence, in the second stage, can deform these small-scale condensations in shape and orient them relative to the background magnetic fields.

Observations and theoretical studies establish that magnetic fields play an important role in shaping the structure and dynamics of molecular clouds and their substructures (e.g. Basu, 2000; Fiege and Pudritz, 2000; Hennebelle, 2003). The relative alignment of the projected magnetic field with the projected minor axis of the condensations is an important diagnostic.

In conformity with the above explanation, Nejad-Asghar and Ghanbari (2003 hereafter NG) interested to investigate the effect of ambipolar diffusion on the thermal instability and formation of small-scale condensations in the magnetic molecular clouds. They concluded that there are solutions where the thermal instability allows compression along the magnetic field but not perpendicular to it. NG inferred that this aspect might be evidence in formation of the observed oblate small-scale condensations in magnetic molecular clouds.

In this paper we want to testify and develop the work of NG by including self-gravity and local background contraction/expansion. We present the basic equations, background evolution, and the linearized equations in Section 2. Section 3 deals with exponential growth rate and parametric solutions that culminates in formation of oblate, prolate, and spherical condensations. Section 4 allocates to a conclusion and some future prospects.

2. The equations of the problem

The basic equations, including self-gravity and ambipolar diffusion, are given first in general (§ 2.1) and then specialized for the homogeneous contracting/expanding molecular cloud (§ 2.2) and for small perturbations to that medium (§ 2.3).

2.1. Equations

In principle, the ion velocity $\boldsymbol{v}_i$ and the neutral velocity $\boldsymbol{v}_n$ in molecular clouds, should be determined by solving separate fluid equations for these species (Draine, 1986), including their coupling by collision processes. But, in the time-scale of cooling considered here, ($10^3 - 10^4 yr$, Gilden, 1984), two fluids of ion and neutral are well coupled together, and we can use the basic equations as follows (Shu, 1992)

$$\frac{d\rho}{dt} + \rho\nabla\cdot\boldsymbol{v} = 0 \tag{1}$$

$$\rho\frac{d\boldsymbol{v}}{dt} + \nabla p + \nabla\left(\frac{B^2}{8\pi}\right) - (\mathbf{B}\cdot\nabla)\frac{\mathbf{B}}{4\pi} + \rho\nabla\psi = 0 \tag{2}$$

$$\frac{1}{\gamma-1}\frac{dp}{dt} - \frac{\gamma}{\gamma-1}\frac{p}{\rho}\frac{d\rho}{dt} + \rho\Omega - \nabla\cdot(K\nabla T) = 0 \tag{3}$$

$$\frac{d\mathbf{B}}{dt} + \mathbf{B}(\nabla\cdot\boldsymbol{v}) - (\mathbf{B}\cdot\nabla)\boldsymbol{v} = \nabla\times\left\{\frac{\mathbf{B}}{4\pi\,\eta\epsilon\rho^{1+\nu}}\times[\mathbf{B}\times(\nabla\times\mathbf{B})]\right\} \tag{4}$$

$$\nabla^2\psi = 4\pi G\rho \tag{5}$$

$$p - \frac{R}{\mu}\rho T = 0 \tag{6}$$

where variables and parameters have their usual meanings and $\eta \approx 2.46\times10^{14}\mathrm{cm}^3.\mathrm{g}^{-1}.\mathrm{s}^{-1}$ is the collision drag in molecular clouds (see McDaniel and Mason, 1973). We use the relation $\rho_i = \epsilon\rho_n^{\nu}$ ($\epsilon \approx 1.83\times10^{-17}\mathrm{cm}^{-3/2}.g^{1/2}$, $\nu = 1/2$) between ion and neutral densities (Umebayasi and Nakano, 1980), and in a good approximation we choose $\rho = \rho_n + \rho_i \approx \rho_n$.

$\Omega(\rho, T) = \Lambda(\rho, T) - \Gamma_{\mathrm{tot}}$ is the net cooling function ($\mathrm{erg.s}^{-1}.\mathrm{g}^{-1}$), where Γ_{tot} is the total heating rate and $\Lambda(\rho, T)$ is the cooling rate which can be written as (Goldsmith and Langer, 1978; Neufeld et al., 1995)

$$\Lambda(\rho, T) = \Lambda_0\rho^{\delta}T^{\beta} \tag{7}$$

where Λ_0, δ, and β are constants. The range of β is 1.4 to 2.9. The constant δ is greater than zero for optically thin case and less than zero for optically thick case (see Fig. 1).

Models of the molecular clouds identify several different heating mechanisms. In this paper, we consider the heating rates of cosmic rays, H_2 formation, H_2 dissociation, grain photoelectrons, and collisions with warm dust, as a constant Γ_0 (Glassgold and Langer, 1974; Goldsmith and Langer, 1978). The heating of the gas by magnetic ion-neutral slip is discussed in detail by Scalo (1977); a simple estimate of this heating rate is

$$\Gamma_{AD} = \eta\epsilon\rho^{\nu}v_d^2 \tag{8}$$

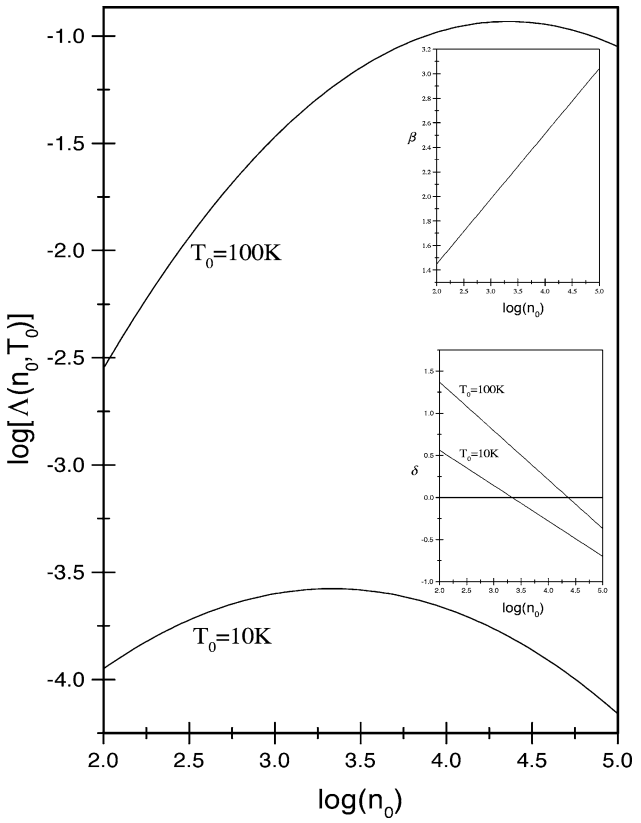

Fig. 1 Logarithm of the cooling rate, $\Lambda(n_0, T_0) = \Lambda_0 n_0^{\delta} T_0^{\beta}$, versus number density in molecular clouds, $n_0(\mathrm{cm}^{-3})$. The values of δ and β are shown in this figure

where v_d is the drift velocity of ions

$$v_d = \frac{1}{4\pi\eta\epsilon\rho^{1+\upsilon}} \mid (\nabla \times \mathbf{B}) \times \mathbf{B} \mid . \tag{9}$$

In order of magnitude, if κB_0 changes on a typical scale of λ, then

$$v_d \sim \frac{(\kappa B_0)^2}{4\pi\eta\epsilon\rho^{1+\nu}\lambda}, \tag{10}$$

and ambipolar diffusion heating rate is given by

$$\Gamma_{AD} = \Gamma_0' \rho^{-(2+\nu)} \tag{11}$$

where Γ_0' is defined as

$$\Gamma_0' \equiv \frac{(\kappa B_0)^4}{16\pi^2\eta\epsilon\lambda^2}. \tag{12}$$

The gravitational heating rate is found by setting the rate of compressional/expansional work per particle, $pd(n^{-1})/dt$, equal to the rate of change of gravitational energy per particle, $[d(\mathrm{PE_{tot}})/dt]/(nV)$, where $\mathrm{PE_{tot}}$ is the gravitational potential energy of the volume V. For a uniform sphere of radius λ, we find

$$\Gamma_{\mathrm{grav}} = \Gamma_0'' \rho^{3/2} \tag{13}$$

where Γ_0'' is defined as

$$\Gamma_0'' \equiv \frac{(4\pi G)^{3/2}}{5\sqrt{3}} [-\dot{a}(\tau)]\lambda^2 \tag{14}$$

where $\dot{a}(\tau)$ is the contraction/expansion parameter rate (see § 2.2).

2.2. Background evolution

As a basis for the small-perturbation analysis, we assume a homogeneous background which is expanding/contracting uniformly, so that the unperturbed quantities only depend on time. The background quantities will be denoted with the subscript 0. The expansion is given by

$$\boldsymbol{r} = a(t)\boldsymbol{x} \tag{15}$$

where $\boldsymbol{r}$ is the Eulerian coordinate, $\boldsymbol{x}$ is the Lagrangian coordinate and $a(t)$ is the expansion/contraction parameter. Using Equation (15), the unperturbed velocity field is given by

$$v_0(\boldsymbol{r}, t) = \frac{da/dt}{a}\boldsymbol{r}. \tag{16}$$

for the background evolution, the basic Equations (1)–(6) reduce to

$$\rho_0(t) = \rho_0(t=0)a(t)^{-3}, \quad p_0(t) = p_0(t=0)a(t)^{-3\gamma}$$
$$T_0(t) = T_0(t=0)a(t)^{-3(\gamma-1)}, \ \mathbf{B}_0(t) = \mathbf{B}_0(t=0)a(t)^{-2} \tag{17}$$

where $a(t)$ follows the differential equation

$$a(\tau)^2\ddot{a}(\tau) = -1 \tag{18}$$

where the dot over the symbol indicates the derivative respect to a non-dimensional variable $\tau \equiv [\frac{4}{3}\pi G\rho_0(t=0)]^{1/2}t$.

2.3. Linearized equations

Density fluctuation ratios in the molecular substructures is in the order of ∼10 (Falgarone et al., 1992; Pan et al., 2001). Therefore, the linear regime of the thermal instability might lead to some significant results for small-scale condensation formation.

To obtain a linearized system of equations, we split each variable into unperturbed and perturbed components, indicating the latter with a subscript 1. Eulerian del operator is

applied to the equations and all equations are rewritten in terms of the Lagrangian coordinate $\boldsymbol{x}$. The resulting linear system has coefficients which depend on t but not on $\boldsymbol{x}$. We then carry out a spatial Fourier analysis, with Fourier components proportional to $\exp(i\boldsymbol{k}\cdot\boldsymbol{x})$, so that $\boldsymbol{k}$ is the Lagrangian wave vector.

Simplifying the resulted linear system by repeated use of the background Equation (17); we obtain

$$\frac{d}{dt}\left(\frac{\rho_1}{\rho_0}\right)+i\tilde{k}\cdot v_1=0 \tag{19}$$

$$\frac{d\mathbf{v}_1}{dt}+\frac{da/at}{a}\mathbf{v}_1+i\frac{c_s}{\gamma\tau_s}\frac{\tilde{\mathbf{k}}}{\tilde{k}}\left(\frac{p_1}{p_0}\right)+i\frac{\mathbf{B}_0\cdot\mathbf{B}_1}{4\pi\rho_0}\tilde{\mathbf{k}} -i\frac{\tilde{\mathbf{k}}\cdot\mathbf{B}_0}{4\pi\rho_0}\mathbf{B}_1-i\frac{\tilde{\mathbf{k}}}{\tilde{k}^2\tau_g^2}\left(\frac{\rho_1}{\rho_0}\right)=0 \tag{20}$$

$$\frac{d}{dt}\left(\frac{p_1}{p_0}\right)+i\gamma\tilde{\boldsymbol{k}}\cdot\boldsymbol{v}_1+\left(\frac{1}{\tau_{c\rho}}+\frac{1}{\tau_K}\right)\left(\frac{p_1}{p_0}\right) +\left(\frac{1}{\tau_{cT}}-\frac{1}{\tau_{c\rho}}-\frac{1}{\tau_K}\right)\left(\frac{\rho_1}{\rho_0}\right)=0 \tag{21}$$

$$\frac{d\mathbf{B}_1}{dt}+i\mathbf{B}_0(\tilde{\boldsymbol{k}}\cdot\boldsymbol{v}_1)-i(\tilde{\boldsymbol{k}}\cdot\mathbf{B}_0)\boldsymbol{v}_1+\frac{2da/dt}{a}\mathbf{B}_1 +\tilde{\boldsymbol{k}}\times\left\{\frac{\mathbf{B}_0}{4\pi\eta\epsilon\rho_0^{1+\nu}}\times[\mathbf{B}_0\times(\tilde{\boldsymbol{k}}\times\mathbf{B}_1)]\right\}=0 \tag{22}$$

where $c_s=\sqrt{\gamma p_0/\rho_0}$ and $\tilde{\boldsymbol{k}}=\boldsymbol{k}/a$ are, respectively, the adiabatic background sound speed and the Eulerian wave vector. The other symbols have the following definitions:

$$\tau_s\equiv\frac{1}{\tilde{k}c_s},\quad \tau_g\equiv\frac{1}{\sqrt{4\pi G\rho_0}},\quad \tau_K\equiv\frac{R\rho_0}{\mu(\gamma-1)K\tilde{k}^2},$$
$$\tau_{cT}\equiv\frac{RT_0}{\mu(\gamma-1)\rho_0(\partial\Omega/\partial\rho)_T},\quad \tau_{c\rho}\equiv\frac{R}{\mu(\gamma-1)(\partial\Omega/\partial T)_\rho}; \tag{23}$$

that are the characteristic time-scale of sound waves, self-gravity perturbation waves, thermal conduction, isothermal and isobaric differential cooling, respectively.

We use the coordinate system $\boldsymbol{u}_x$, $\boldsymbol{u}_y$, and $\boldsymbol{u}_z$ as specified by NG. Equations (20) and (22) may be used to uncouple v_{1y}- the perturbed velocity in the plane perpendicular to both $\mathbf{B}_0$ and $\boldsymbol{k}$- from the rest of the problem. With the choice of exponential perturbation (e^{ht}), disturbances perpendicular to the $(\mathbf{B}_0-\boldsymbol{k})$-plane, have a solution which displays existence or non-existence of the Alfvén waves. Amplitude of the Alfvén waves are damped via expansion of the medium and/or with ion-neutral friction, while, it must grow with injection of energy in contracting medium.

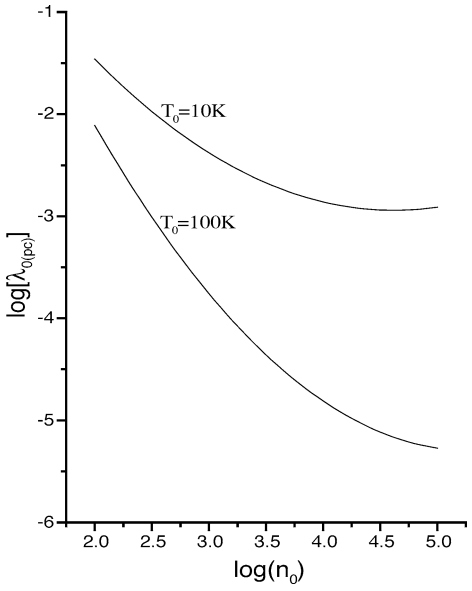

Fig. 2 Logarithm of the Field length (at unit of parsec) in the typical molecular clouds versus number density, $n_0(\mathrm{cm}^{-3})$

The motion in the other modes are constrained to the xz-plane, and are governed by the matrix equation,

$$Y^{(1)}=AY \tag{24}$$

where Y is a 5×1 matrix as

$$Y=\begin{pmatrix}\rho_1/\rho_0\\ p_1/p_0\\ av_{1x}\\ av_{1z}\\ \sin\theta\left(\frac{B_{1z}}{B_0}\right)-\cos\theta\left(\frac{B_{1x}}{B_0}\right)\end{pmatrix},$$

and $Y^{(1)}$ is its first time derivative. The 5×5 matrix of the coefficients, A, is defined as

$$A=\begin{pmatrix}0 & 0 & -\frac{i\sin\theta}{c_s\tau_s a} & -\frac{i\cos\theta}{c_s\tau_s a} & 0\\ \frac{1}{\tau_{c\rho}}+\frac{1}{\tau_K}-\frac{1}{\tau_{cT}} & -\frac{1}{\tau_{c\rho}}-\frac{1}{\tau_K} & -\frac{i\gamma\sin\theta}{c_s\tau_s a} & -\frac{i\gamma\cos\theta}{c_s\tau_s a} & 0\\ \frac{ic_s\tau_s a\sin\theta}{\tau_g^2} & \frac{ic_s a\sin\theta}{\gamma\tau_s} & 0 & 0 & -\frac{ic_s\tau_s a}{\tau_{AL}^2}\\ \frac{ic_s\tau_s a\cos\theta}{\tau_g^2} & \frac{ic_s a\cos\theta}{\gamma\tau_s} & 0 & 0 & 0\\ 0 & 0 & -\frac{i}{c_s\tau_s a} & 0 & -\frac{1}{\kappa^2\tau_{AD}}\end{pmatrix},$$

where θ is the angle between $\boldsymbol{k}$ and $\mathbf{B}_0$, and

$$\tau_{AL}\equiv\frac{1}{\tilde{k}v_A}=\frac{\sqrt{4\pi\rho_0}}{\tilde{k}B_0},\quad \tau_{AD}\equiv\frac{1}{\tilde{k}v_d}=\frac{4\pi\eta\epsilon\rho_0^{1+\nu}}{\tilde{k}^2(\kappa B_0)^2} \tag{25}$$

are the characteristic time-scales of the Alfvén waves and ambipolar diffusion, respectively.

3. Exponential growth rate

The standard exponential growth rate provides the following formal solution for all the perturbations:

$$y_i(t) = y_i(t = 0)\exp(ht), \tag{26}$$

where real(h) represents the growth/decay rate. Inserting the background evolution Equation ([17]) and exponential growth form (Equation [26]), into Equation (24); we obtain

$$Y^{(1)} = hY + CY \tag{27}$$

where C is a diagonal matrix as

$$C \equiv \frac{1}{\tau_e}\text{diag}[3, 3\gamma, 1, 1, 2] \tag{28}$$

where $\mid \tau_e \mid = \frac{a}{\mid da/dt \mid}$ represent contraction/expansion time-scale. Existence of solution for Equation (27), needs the following condition:

$$\text{Det}[hI + C - A] = 0 \tag{29}$$

where I is the unitary matrix. By introducing the non-dimensional quantities

$$y \equiv h\tau_s,\ \sigma_\rho \equiv \frac{\tau_s}{\tau_{cT}},\ \sigma_T \equiv \frac{\tau_s}{\tau_{c\rho}} + \frac{\tau_s}{\tau_K},$$
$$\alpha \equiv \left(\frac{\tau_s}{\tau_{AL}}\right)^2,\ D \equiv \frac{\tau_s}{\kappa^2\tau_{AD}},\ G_g \equiv \left(\frac{\tau_s}{\tau_g}\right)^2,\ E_e \equiv \frac{\tau_s}{\tau_e}, \tag{30}$$

we find a five-degree linear characteristic Equation that without self-gravity and expansion/contraction of the background ($G_g = 0$, $E_e = 0$), reduces to the Equation (22) of NG. We use the Laguerre method to find the roots of this characteristic equation.

3.1. The sound domain

When the sound period, τ_s, is much smaller than the other characteristic time-scales, we can neglect the effect of α, D, G_g, and E_e. The characteristic Equation reduces to a three-degree linear Equation. There are three solutions: two sound waves and one condensation mode. The stable region for this case is shown in the Fig. 1 of NG.

For the temperatures and densities that thermal instability is destabilizing, there exist a critical length (Field length) defined as the maximum wavelength which thermal conduction can suppress the instability. Inserting the defined time-scales (Equation [23]), into the definitions of σ_ρ and σ_T; we obtain

$$\sigma_\rho = \frac{\mu(\gamma - 1)}{RT_0\tilde{k}c_s}\Lambda(n_0, T_0)(\delta + 2.5\xi - 1.5\chi) \tag{31}$$

$$\sigma_T = \frac{\mu(\gamma - 1)}{RT_0\tilde{k}c_s}\Lambda(n_0, T_0)\beta\left[1 + \left(\frac{\lambda_0}{\lambda}\right)^2\right] \tag{32}$$

where ξ and χ are

$$\xi \equiv \frac{\Gamma_{AD}}{\Lambda(n_0, T_0)},\quad \chi \equiv \frac{\Gamma_{\text{grav}}}{\Lambda(n_0, T_0)} \tag{33}$$

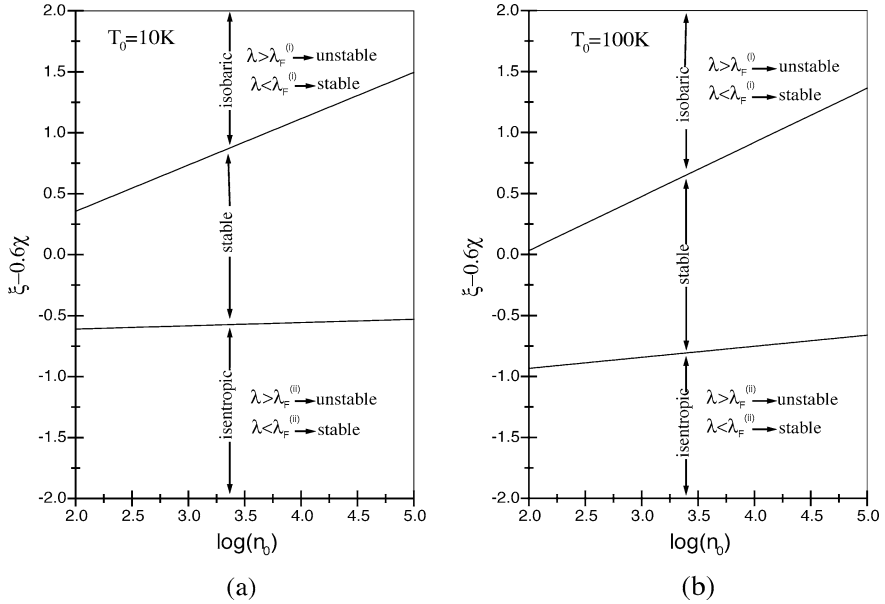

Fig. 3 The stable, isobaric instability, and isentropic instability of the medium which can occur according to the different values of $\xi - 0.6\chi$, for (a) $T_0 = 10K$ and (b) $T_0 = 100K$

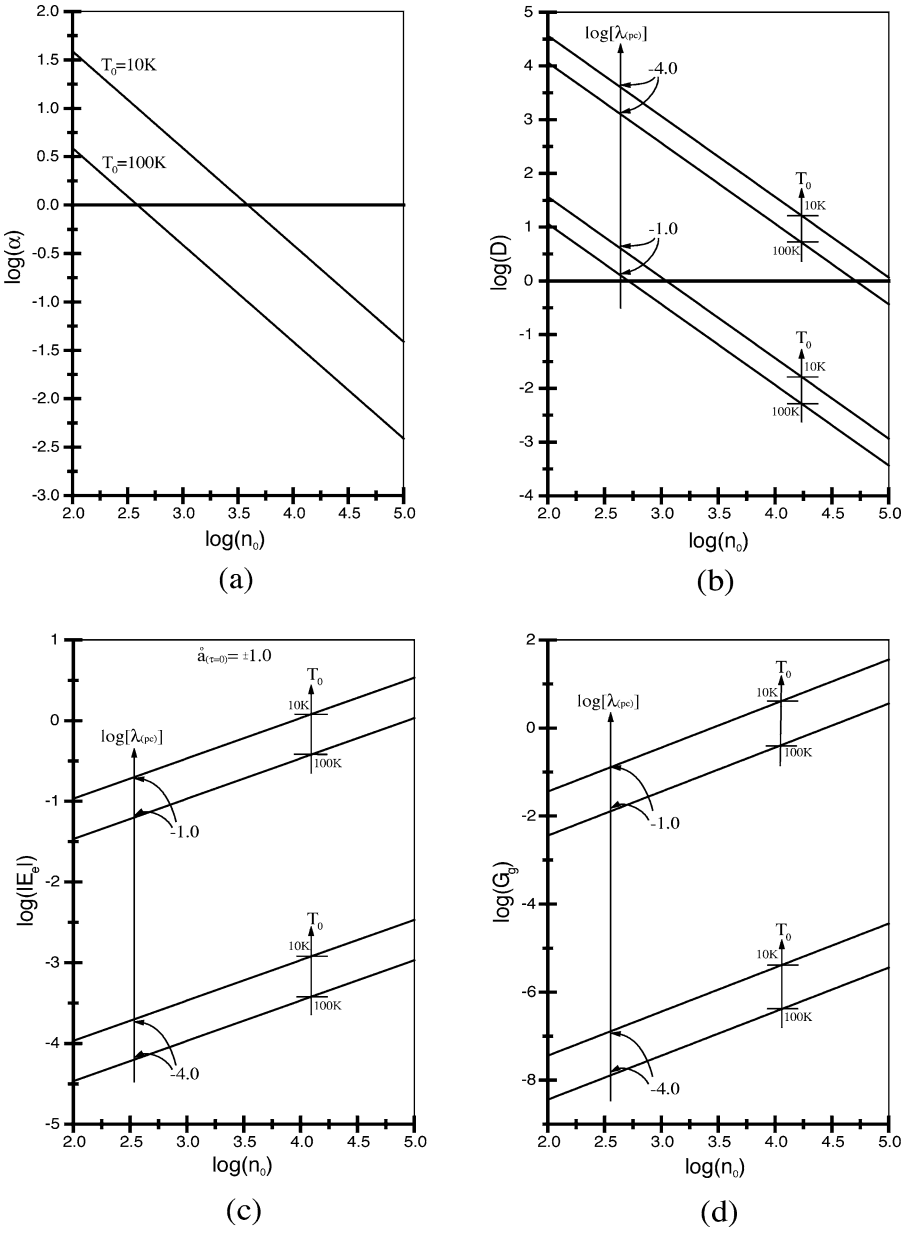

Fig. 4 The typical values of α, D, E_e, and G_g in molecular clouds

and λ_0 is a defined wavelength as follows:

$$\lambda_0 \equiv \sqrt{\frac{K T_0}{\beta n_0 \Lambda(n_0, T_0)}}. \tag{34}$$

The values of the $\lambda_{0(pc)}$ for typical data in the molecular clouds is given in Fig. 2. According to this figure, we choose wavelengths in the range of $\lambda_{(pc)} \approx 10^{-4} - 10^{-1}\, pc$, that are interesting in formation of the small-scale condensations.

We can now define a generalized Field length for two cases as follows:

- $\delta + 2.5\xi - 1.5\chi > \beta$, which $\sigma_\rho > 0$, that is upwards of the $\sigma_T - \sigma_\rho$ plane:

$$\lambda_F^{(i)} = \frac{\lambda_0}{\sqrt{\dfrac{\delta + 2.5\xi - 1.5\chi}{\beta} - 1}} \tag{35}$$

- $\delta + 2.5\xi - 1.5\chi < -\frac{2}{3}\beta$, which $\sigma_\rho < 0$, that is downwards of the $\sigma_T - \sigma_\rho$ plane:

$$\lambda_F^{(ii)} = \frac{\lambda_0}{\sqrt{\frac{3}{2}\dfrac{1.5\chi - \delta - 2.5\xi}{\beta} - 1}}. \tag{36}$$

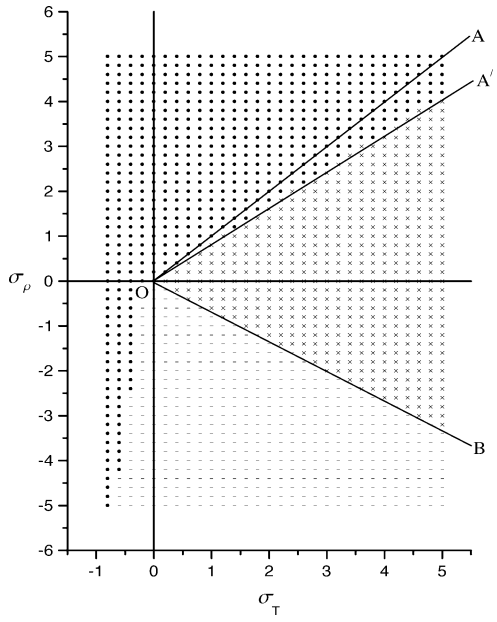

Fig. 5 Regions of stability(×), spherical instability(•), and oblate instability(−) for the case of $G_g = 0.1$ and $E_e = 0$, for a typical value of $\alpha = 5.0$ and $D = 1.0$. The decreased stability region in the isobaric instability criterion (line OA), occurs by the increasing of internal pressure via existence of self-gravity

If $\delta + 2.5\xi - 1.5\chi$ sets between $-\frac{2}{3}\beta$ and β, the Field length can not be defined, thus, the medium is stable for all wavelengths. Otherwise, for wavelengths greater than the defined Field lengths (equation [35] and [36]), the medium is unstable. This case is shown in Fig. 3 for two temperatures of $10K$ and $100K$.

Before proceeding any further, we must have a real physical feeling of defined non-dimensional parameters: α, D, E_e, and G_g. We consider some typical magnetic molecular clouds with density between 10^2cm^{-3} to 10^5cm^{-3}, temperatures in the range of $T_0 \approx 10 - 100K$, and magnetic field strength $B_0 \approx 10\mu G$ (Myers and Goodman, 1988, Crutcher, 1999). The typical values of α, D, E_e, and G_g are shown in Fig. 4.

3.2. The magnetic domain

Wherever the Alfvén period and the ambipolar diffusion time-scale are important in the magnetic molecular clouds, we can not ignore the effect of α and D in the characteristic Equation. This case has recently been investigated by NG, without self-gravity and local expansion/contracion of the background ($G_g \approx 0$, $E_e \approx 0$). They conclude that there are solutions where the thermal instability allows compression along the magnetic field but not perpendicular to it (see Fig. 2 and Fig. 4 of NG). Maximum effect of the magnetic domain for the oblate condensation formation is occurred when ambipolar diffusion time-scale is nearly equal to the period of sound waves $D \approx 1.0$ (i.e. $\tau_s \approx \kappa^2 \tau_{AD}$).

3.3. The self-gravity and expansion/contraction domain

In this subsection we investigate the effect of the self-gravity and the expansion/contraction of background. If we consider the effect of the self gravity without expansion/contraction of the background, the isobaric instability criterion (line OA of Fig. 1 of NG) is modified via bringing this line downwards. This case is shown in Fig. 5, for a typical value of $\alpha = 5.0$ and $D = 1.0$. Physically, this means that self-gravity causes to increase the internal pressure, thus, isobaric instability must occur at a decreased σ_ρ for each σ_T.

If the background is expanding ($E_e > 0$), its expansion energy causes to stabilize the medium. This case is shown in Fig. 6 for a typical value of $\alpha = 5.0$ and $D = 1.0$. In the isentropic instability criterion (line OB), expansion energy causes to stabilize the medium in the direction of the magnetic field and perpendicular to it. On the other hand, in the isobaric instability criterion (line OA), it only causes to stabilize the medium in perpendicular to the magnetic field, corresponding to decreased pressure via ion-neutral friction.

For contracting background ($E_e < 0$), contraction energy injected to the medium, thus, its stability is decreased and converted to a prolate instability. Diffusion of neutrals relative to the freezed ions in the perpendicular direction of the magnetic field is the reason of this prolate instability. This case is shown in Fig. 7 for a typical value of $\alpha = 5.0$ and $D = 1.0$. When the parameters of a magnetic molecular cloud set, locally, in this region of $\sigma_T - \sigma_\rho$ plane, prolate condensation may be produced via thermal instability.

4. Summary and prospects

In this paper we perform linear analysis of thermal instability in a locally uniform expanding/contracting magnetic molecular clouds which, in the perturbed state, is undergoing ambipolar diffusion. Thermal conduction and self-gravity have also been included as fundamental ingredients. The small-perturbation problem yields a system of ordinary differential Equations with five independent solutions. We choose an exponential growth rate which convert the system of ordinary differential Equations into a five-degree complete characteristic Equation. If we neglect the self-gravity and expansion/contraction of the background, the characteristic Equation reduces to the prior results of NG. We have used the Laguerre method to find the roots of this complete characteristic equation.

In sound domain, two of the solutions have the character of oscillatory modes (sound waves) and the third one is a non-oscillatory (or condensation) solution. We adopt a para-

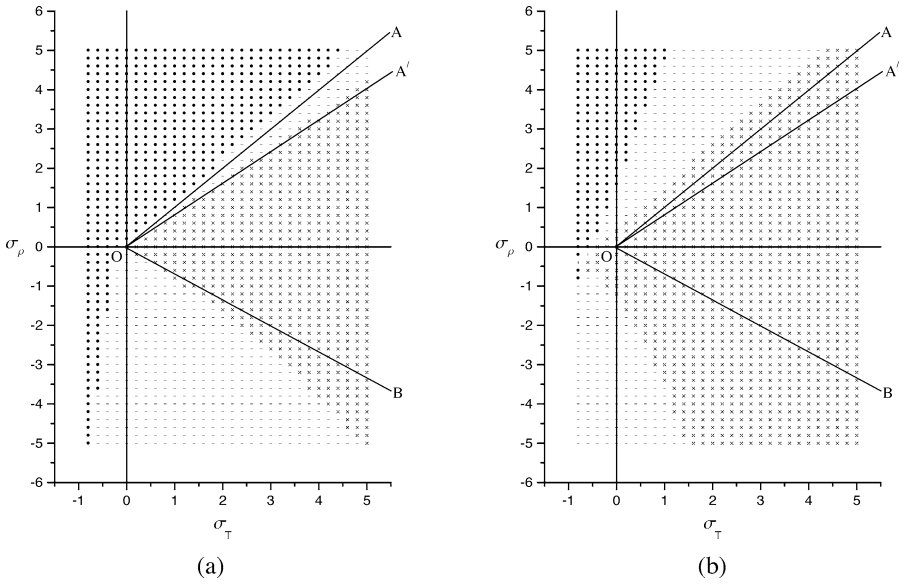

Fig. 6 Regions of stability($\times$), spherical instability($\bullet$), and oblate instability($-$) in the expanding background, for a typical value of $\alpha = 5.0$ and $D = 1.0$, with (a) $E_e = 0.01$ and $G_g = 0.1$, and (b) $E_e = 0.1$ and $G_g = 0$

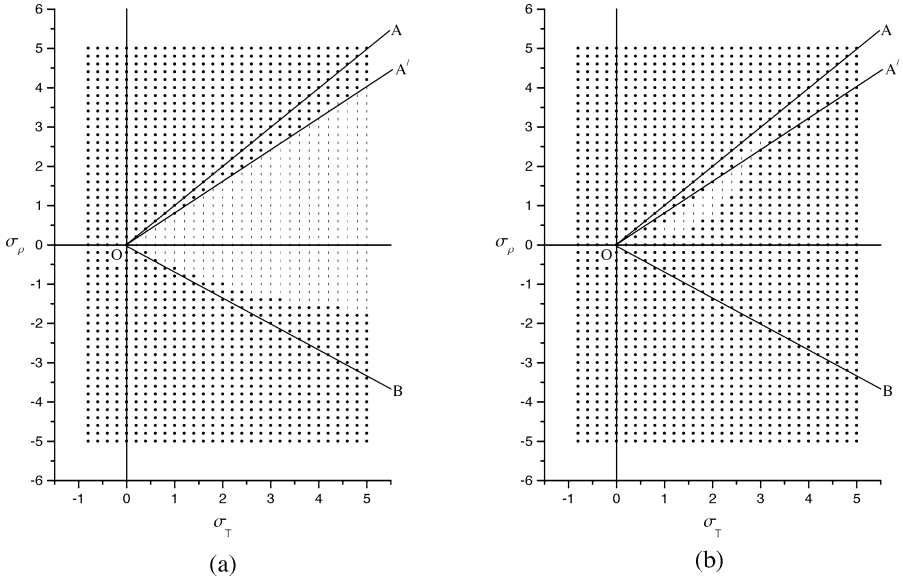

Fig. 7 Regions of spherical instability($\bullet$), and prolate instability(|) in the contracting background, for a typical value of $\alpha = 5.0$ and $D = 1.0$, with (a) $E_e = -0.01$ and $G_g = 0.1$, and (b) $E_e = -0.1$ and $G_g = 0$

metric net cooling function and find for perturbations with wavelengths greater than the Field length, thermal instability causes the medium to condense. Figure 3 shows the condition of instability in the molecular clouds which their cooling rates are presented in Fig. 1.

We choose a wide range of density and temperature in the molecular clouds with typical magnetic field strength $B_0 \approx 10\mu G$. Interesting wavelengths in the problem are around the Field length which is shown in Fig. 2. According to this figure, we consider wavelengths around $10^{-4} - 10^{-1} pc$ for small-scale condensations. The typical values of α, D, E_e, and G_g are shown in Fig. 4.

In magnetic domain, without self-gravity and expansion/contraction of the background, there are solutions where the thermal instability allows compression along the magnetic field but not perpendicular to it. Maximum cases of these oblate condensation solutions are occurred when the ambipolar diffusion time-scale equals to the period of sound waves ($D \approx 1$).

Figures 5 to 7 show results that come into existence by considering of self-gravity and local expansion/contraction of the magnetic molecular cloud. We deduce that the self-gravity causes to increase the internal pressure, thus, isobaric instability must occurs at a decreased σ_ρ for each σ_T. Therefore, instability of the medium is increased. In the expanding background, expansion energy in the isentropic instability, causes to stabilize the medium in the direction of the magnetic field and perpendicular to it, while, in the isobaric instability it only stabilize the medium in the perpendicular direction. In the contracting background, stability of the medium is de-

creased and converted to the prolate instability via injection of contraction energy and diffusion of free neutrals relative to freezed ions.

In this paper we conclude that linear thermal instability can produce small-scale condensations in spherical, oblate, or prolate. We try to analyze a rather involved problem linearly, because, before this process overcome, *turbulence* causes to interaction and merging of these newly formed condensations. Physically, we expect that merging of these small-scale condensations culminate in the large-scale clumps that are star bearing regions in our world. Authors are now preparing a complete simulated turbulent magnetic molecular cloud with condensations produced by thermal instability. It would be interested to investigate the effect of interaction, merger, and coagulation of these small-scale condensations with smoothed particle hydrodynamics (SPH) method.

References

Arons, J., Max, C.E.: ApJ **196**, L77 (1975)
Basu, S.: ApJ **540**, L103 (2000)
Crutcher, R.M.: ApJ **520**, 706 (1999)
Draine, B.T.: MNRAS **220**, 133 (1986)
Falgarone, E., Puget, J.L., Pérault C.K.: A&A **257**, 715 (1992)
Fiege, J.D., Pudritz, R.E.: ApJ **534**, 291 (2000)
Gammie, C.F., Lin Y., Stone, J.M., Ostriker, E.C.: ApJ **592**, 203 (2003)
Gilden, D.L.: ApJ **283**, 679 (1984)
Glassgold, A.E., Langer, W.D.: ApJ **193**, 73 (1974)
Goldsmith, P.F., Langer, W.D.: ApJ **222**, 881 (1978)
Hartmann, L.: ApJ **578**, 914 (2002)
Hennebelle, P.:, A&A, **397**, 381 (2003)
Indebetouw, R., Zweibel E.G.: ApJ **532**, 361 (2000)
Jones, C.E., Basu, S.: ApJ **569**, 280 (2002)
Larson, R.B.: MNRAS **194**, 809 (1981)
Liszt, H., Lucas, R.: A&A **355**, 333 (2000)
McDaniel, E.W., Mason, E.A.: The Mobility And Diffusion of Ions in Gases, New York: Wiley, p.127 (1973)
Moore, E.M., Marscher, A.P.: ApJ **452**, 679 (1995)
Myers, P.C., Goodman, A.A.: ApJ **329**, 392 (1988)
Nejad-Asghar, M., Ghanbari, J.: MNRAS **345**, 1323 (NG) (2003)
Nelson, R.P., Langer, W.D.: ApJ **482**, 796 (1997)
Neufeld, D.A., Leep, S., Melnick, G.J.: ApJS **100**, 132 (1995)
Pan, K., Federman, S.R., Welty, D.E.: ApJ **558**, L105 (2001)
Peng, R., Langer, W.D., Velusamy, T., Kuiper, T.B.H., Levin, S.: ApJ **497**, 842 (1998)
Rollinde, E., Boissé, P., Federman, S.R., Pan, K.: A&A **401**, 215 (2003)
Ryden, B.S.: ApJ **471**, 822 (1996)
Sakamoto, S., Sunada, K.: ApJ **594**, 340 (2003)
Scalo, J.M. ApJ **213**, 705 (1977)
Shu, F.: The Physics of Astrophysics, Vol II. University Science Books, Mill Valley, CA p.360 (1992)
Solomon, P.M., Rivolo, A.R., Barrett, J., Yahil, A.: ApJ **319**, 730 (1987)
Umebayashi, T., Nakano T.: PASJ **32**, 405 (1980)